

Quantum Chemical Studies on ZrN Nanostructures

V. Nagarajan and R. Chandiramouli*

School of Electrical & Electronics Engineering
SASTRA University, Tirumalaisamudram, Thanjavur -613 401, India

*Corres. Author: rcmouli@gmail.com
Tel: +919489566466, Fax.:+91-4362-264120

Abstract: The realistic ZrN nanostructures namely ZrN nanocube-4, nanocube-6, nanocube-8, nanosheet-12 and buckycage-10 are constructed and optimized using density functional theory utilizing B3LYP/LanL2DZ basis set. ZrN nanostructures stability is studied using calculated energy, binding energy and vibrational studies. The dipole moment and point symmetry are discussed. The electronic properties of ZrN nanostructures are invoked with HOMO-LUMO gap, ionization potential and electron affinity. The embedding energy gives the insight to incorporate the foreign atom in the nanostructure. The stability and electronic properties of nanostructures leads to tailor new materials of ZrN with enhanced properties.

Keywords: Zirconium nitride, nanostructures, electronic properties, HOMO-LUMO, embedding energy.

Introduction

Zirconium nitride (ZrN) exhibit sodium chloride crystal structure, space group of ZrN is Fm3m with lattice parameter of 4.57 Å. ZrN possess different properties such as metallic like thermal and electronic conduction, which seems to be similar to most ceramics, it exhibits very hard and brittle nature [1, 2]. In its structure zirconium occupies face centered cubic (FCC) lattice with nitrogen in the octahedral interstices, forming its own FCC sublattice. The presence of nitrogen atom with different stoichiometry gives rise to altered physical properties [1]. ZrN shows interesting optical, electrical and structural properties which are related with nitrogen stoichiometry. ZrN shows material transition from stable metallic ZrN to metastable semi-transparent insulating Zr₃N₄ [3]. The transition metal nitrides find its potential applications in refractory material [4], hard coating for cutting tools [5] and Josephson junction in electronics [6]. ZrN nanoparticles are synthesized by ball milling process [7] and benzene-thermal method [8]. Due to the mechanical properties, ZrN has much attention in hard coatings, coatings for improved corrosion resistance and diffusion barriers in microelectronic devices [9-11].

The motivation behind the work is tailoring the proper structure of ZrN leads to improved structural stability and electronic properties of ZrN nanostructures. With this as motivation, the literature survey was conducted and from the survey it is inferred that most of the reported work deals with the synthesis and characterization of ZrN. In the present work, realistic nanostructures of ZrN are constructed and optimized using density functional theory (DFT) [12]. DFT is a better approach to optimize the nanostructures of ZrN precisely to fine-tune its properties.

Computational Details

The nanostructures of ZrN are completely optimized using NWChem package [13]. Density functional theory is a better choice to compute the ground states of atoms in the nanostructures that is based on the electron density functionals. The DFT is implemented by Becke's three-parameter hybrid function (B3LYP) with LanL2DZ basic set [14-18]. LanL2DZ basic set is preferred basis set since it is applicable for the elements such as H, Li-La and Hf-Bi gives the best results with the pseudo potential approximation [19]. Since zirconium has an atomic number of 40 and nitrogen has the atomic number of 7, LanL2DZ is a suitable basis set to optimize the nanostructures. In the present work, different nanostructure of ZrN are simulated and optimized successfully by using NWChem package with LanL2DZ basic set.

Results And Discussion

Structures of ZrN

The present work mainly concerns with calculated energy, dipole moment, HOMO-LOMO gap, ionization potential (IP), electron affinity (EA), binding energy, embedding energy and vibrational studies of ZrN nanostructures. Five different structures of ZrN are constructed and studied namely, ZrN nanocube-4, ZrN nanocube-6, ZrN nanocube-8, ZrN nanosheet-12 and ZrN buckycage-10 are shown in the Figure. 1(a) – 1(e) respectively. In the case of ZrN nanocube-4, there are four Zr atoms and four N atoms forming a cube structure. Looking at the ZrN nanocube-6, six Zr atoms and six N atoms forms an extended cube structure. The structure of ZrN nanocube-8 has eight Zr and eight N atoms forming a cube structure. ZrN nanosheet-12 has twelve Zr and twelve N atoms forming a sheet like two dimensional structure. The ZrN buckycage-10 has ten Zr atoms and ten N atoms forming a three dimensional bucky ball like structure.

Figure.1(a) Structure of ZrN nanocube-4

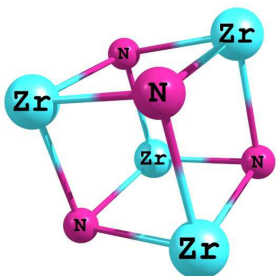


Figure.1(b) Structure of ZrN nanocube-6

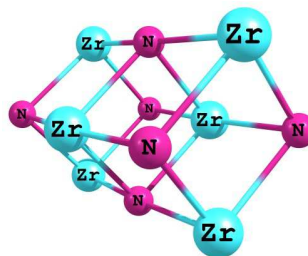


Figure.1(c) Structure of ZrN nanocube-8

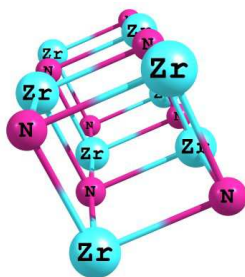
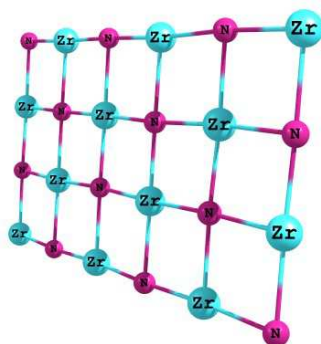
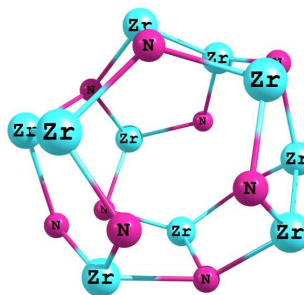


Figure.1(d) Structure of ZrN nanosheet-12**Figure.1(e)** Structure of ZrN buckycage-10

The calculated energy for ZrN nanocube-4 is found to be -405.46 Hartrees. For ZrN nanocube-6 it is calculated to be -608.27 Hartrees. The stability increases for ZrN nanocube-8 with the energy of -811.10 Hartrees. From all the nanocube structures it implies that upon addition of atoms in the structures leads to increase in the stability of the structure. The same is also true for ZrN buckycage-10 which has the energy of -1012.88 Hartrees and ZrN nanosheet-12 has energy of -1216.54 Hartrees. Initially in the premature stage; the stability is low and with increase in the number of atoms the stability increases. Dipole moment (DM) arises due to the unequal distribution of charges inside the nanostructures. The high value of dipole moment indicates that the charges inside the structure are not properly balanced. In nanocube structure the DM is found to be low and varies only between 0.23 – 0.65 Debye due to the well packed atoms in the structure. In contrast, DM for bucky cage-10 is more which 2.1 Debye. This structure is a 3D structure with protruding atoms inside the buckycage leads to high value of DM. In the case of nanosheet which is 2D structure the DM moment is more due to arrangement of atoms with two dimensional structure. The point group for all the structures is found to be C_1 which infers the high order of asymmetry. Table 1 represent the Energy, Dipole moment and Point group of ZrN nanostructures.

Table.1 Energy, Dipole moment and Point group of ZrN Nanostructures

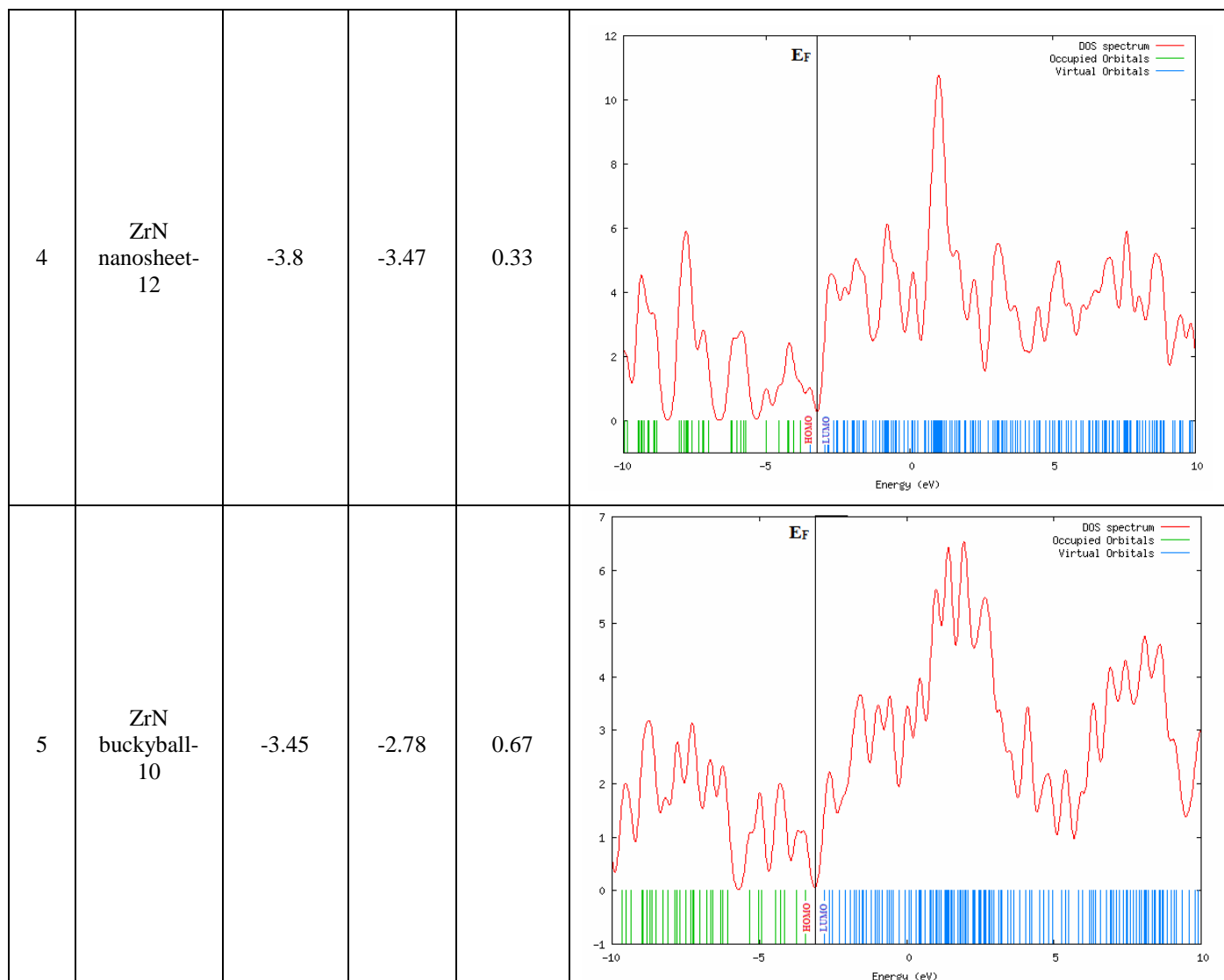
Structure	E (Hartrees)	DM (Debye)	Point group
ZrN nanocube-4	-405.46	0.23	C_1
ZrN nanocube-6	-608.27	0.65	C_1
ZrN nanocube-8	-811.10	0.45	C_1
ZrN nanosheet-12	-1216.54	1.87	C_1
ZrN buckyball-10	-1012.88	2.10	C_1

HOMO-LUMO gap of ZrN nanostructures

The electronic properties of ZrN nanostructures can be invoked with the highest occupied molecular orbital (HOMO) and lowest unoccupied molecular orbital (LUMO) [20,21]. The HOMO-LUMO gap for ZrN nanocube-6 is found to be around 1.31 eV, this means to move the electron from the HOMO level to LUMO level requires more energy. A wide gap requires more energy and narrow gap requires less energy to move the electron from HOMO level to LUMO level. Interestingly, all the other structures except nanocube-6 have a narrow gap in the order of 0.33-0.83 eV. Looking at the density of states (DOS) spectrum which gives the information about the localization of charges within the energy interval indicates that the localization of charges in the conduction band is more compared with valence band. Near the Fermi energy (E_F) the localization of charge is seen more which implies that small energy is sufficient to move the electrons from valence band to conduction which is also in agreement with the HOMO-LUMO gap. Table 2 represents the HOMO-LUMO gap and DOS spectrum of ZrN nanostructures.

Table. 2 HOMO, LUMO and DOS Spectrum of ZrN nanostructures.

Sl. No.	Structure	HOMO (eV)	LUMO (eV)	Gap E_g (eV)	HOMO, LUMO and DOS Spectrum
1	ZrN nanocube-4	-3.09	-2.32	0.77	
2	ZrN nanocube-6	-4.19	-2.88	1.31	
3	ZrN nanocube-8	-3.06	-2.23	0.83	



Ionization potential and Electron affinity of ZrN nanostructures

The ionization potential (IP) and electron affinity (EA) gives the perception for the electronic properties of ZrN nanostructures [22]. EA has more importance in the Plasma Physics and Chemistry and gas discharge. EA also plays an important role in chemical sensors. The IP and EA trend is found to be almost same for all the structures. IP and EA value is more for ZrN nanocube-6 and ZrN nanosheet-12, this arise due to the positions of atoms in the structures. For nanocube-4 and nanocube-8 the value is low and for bucky cage-10 the value is moderate. The structures with high value of EA are suitable for chemical sensors. Figure. 2 depict the IP and EA values of ZrN nanostructures.

Binding energy and Embedding energy of ZrN nanostructures

The binding energy (BE) per atom of ZrN nanostructures are calculated by equation 1,

$$BE = [(n * E(Zr) + n * E(N) - n * E(ZrN)) / n] \text{ ----- (1)}$$

where $E(Zr)$ is the energy of Zr atom, $E(N)$ is the energy of N atom, $E(ZrN)$ is the energy of the ZrN nanostructure and n is the number of atoms present in the structure. BE also provides the information about the stability of the structure [23, 24]. High value of BE indicates the stable structure. BE of all the structure seems to be almost same except bucky cage-10. The high value is due to the overlapping of orbitals between Zr and N atoms in the structure which leads to the stability of the structure. Figure. 3 refers the BE of ZrN nanostructures.

The embedding energy (EE) is used to study how far the foreign atoms can be incorporated in the structure [25]. A high value of EE infers that it requires more energy to embed foreign atom and low value of EE implies less energy is required to embed the substitution impurity. EE is given by equation 2 as,

$$EE = [(n * E(Zr) + n * E(N) - n * E(ZrN))] \text{ ----- (2)}$$

Among all the structures nanocube-4 has low value of EE which is easy to include a foreign atom, in contrast, nanosheet-12 has high value of EE that is difficult to embed the foreign atoms in the structure. Figure. 4 indicate the EE of ZrN nanostructures.

Figure.2 Ionization potential and Electron affinity of ZrN nanostructures

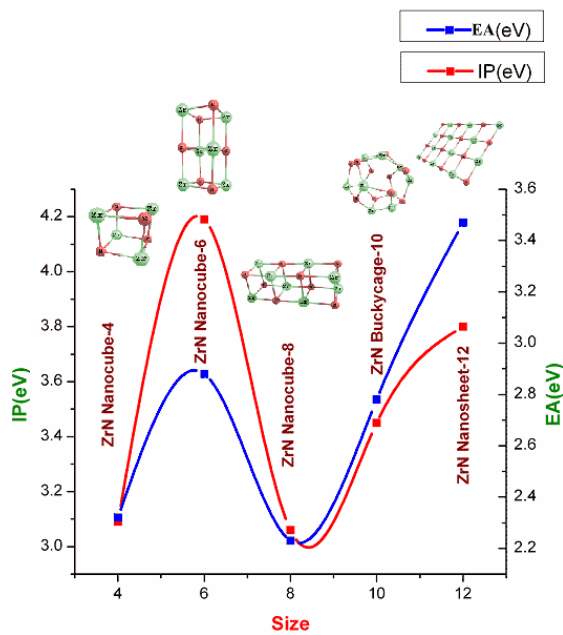


Figure.3 Nanostructures size vs Binding Energy.

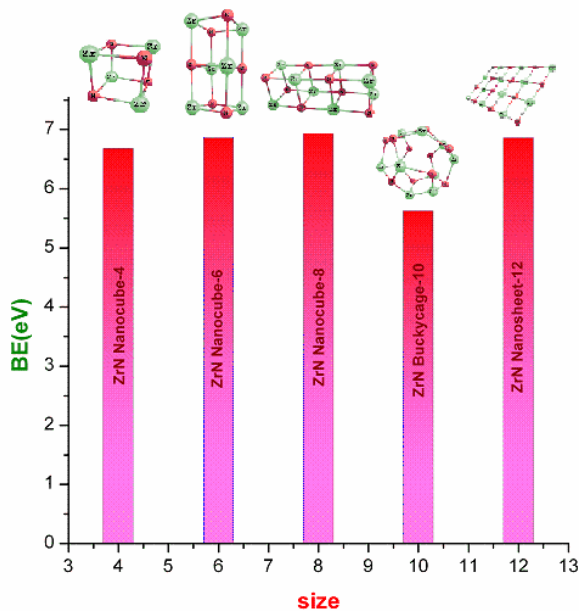
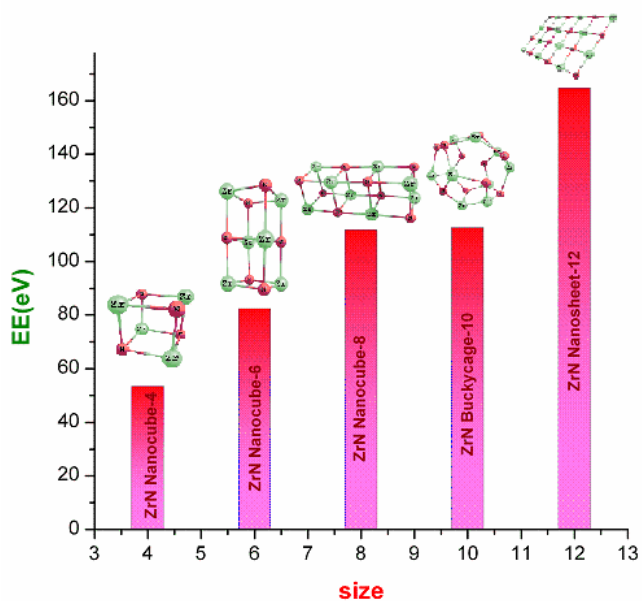


Figure.4 Nanostructures size vs Embedding Energy.

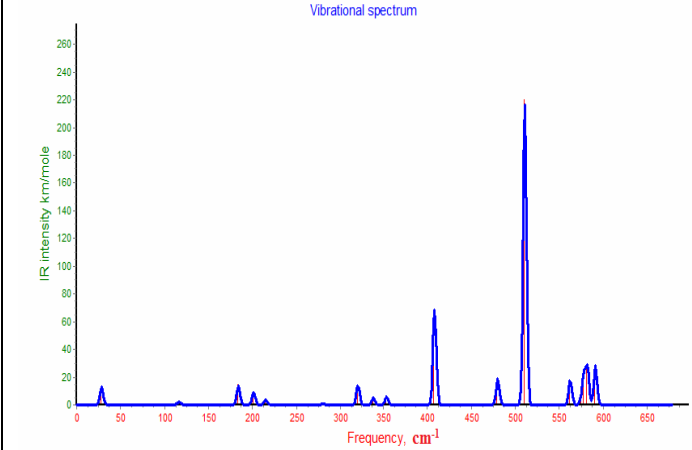
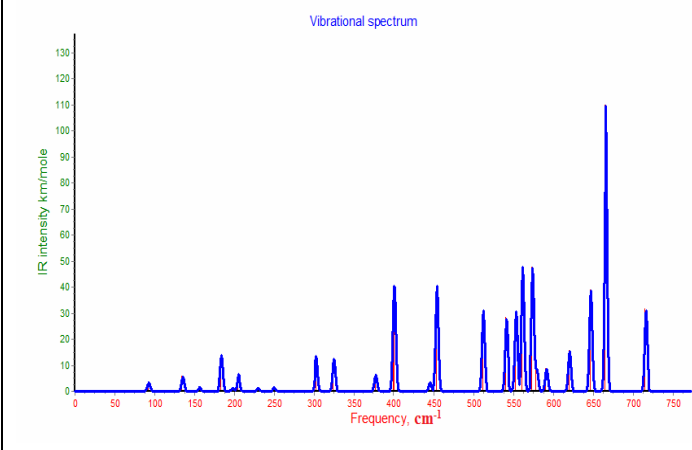
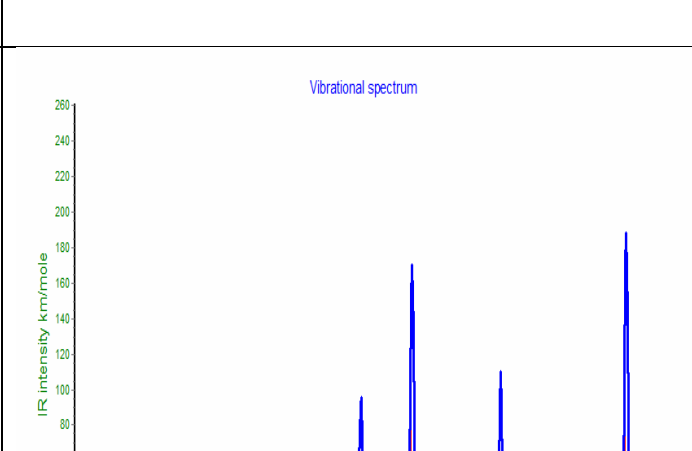
Vibrational Studies of ZrN nanostructures

The vibrational studies provide the stability of nanostructures. The structure with no imaginary frequencies are said to be more stable [26]. Table. 3 represent the vibrational frequency and IR intensity of ZrN nanostructures. For ZrN nanocube-4, the prominent vibrational frequency is seen at 510.94 and 408.23 cm^{-1} which has the IR intensity of 219.78 and 68.57 km/mole respectively. In the case of nanocube-6, the vibrational frequencies are observed at 665.91 and 574.30 cm^{-1} for IR intensity of 109.33 and 47.77 km/mole respectively. ZrN nanocube-8 has the vibrational frequency of 711.06 and 435.49 cm^{-1} with the IR intensity of 126.43 and 113.05 km/mole is observed. In the case of nanosheet-12, IR intensity of 294.02 and 148.60 km/mole is noticed at the vibrational frequency of 541.8 and 546.92 cm^{-1} respectively. ZrN bucky cage-10 has IR intensity of 146.02 and 87.18 km/mole for the vibrational frequency of 311.96 and 1407 cm^{-1} respectively.

Conclusion

The realistic ZrN nanostructures are completely optimized using DFT utilizing B3LYP/LanL2DZ basis set. The stability of the ZrN nanostructures is analyzed using calculated energy, binding energy and vibrational studies. The electronic properties are discussed in terms of HOMO-LUMO gap, IP and EA. The stability depends upon the number of atoms in the structures, when the atoms in the structure increases the stability of the structure also increases. The dipole moment and point symmetry of nanostructures are discussed for different nanostructures. The embedding energy provides the information about the incorporation of foreign atoms in the nanostructures. The information reported in the present work will give an insight to tailor a suitable ZrN nanostructure with enhanced electronic properties which finds its potential applications in hard coatings and microelectronic devices.

Table.3 Vibrational Frequency and IR Intensity of ZrN nanostructures.

Structure	Vibrational Frequency Cm^{-1}	IR Intensity km/mole	Mode assignment	IR spectrum
ZrN Nano cube-4	510.94	219.78	Molecular stretching	 <p>Vibrational spectrum</p> <p>IR intensity km/mole</p> <p>Frequency, cm^{-1}</p>
	408.23	68.57		
ZrN Nano cube-6	665.91	109.83	Molecular stretching	 <p>Vibrational spectrum</p> <p>IR intensity km/mole</p> <p>Frequency, cm^{-1}</p>
	574.30	47.77		
ZrN Nano cube-8	711.06	126.43	Molecular stretching	 <p>Vibrational spectrum</p> <p>IR intensity km/mole</p> <p>Frequency, cm^{-1}</p>
	435.49	113.05		

ZrN Nano sheet-12	541.8	294.02	Molecular stretching	
	546.92	148.60		
ZrN Buckyball-10	311.96	146.02	Molecular stretching	
	1407.00	87.18		

References

1. Toth L.E: “Transition Metal Carbides and Nitrides No. 7 in Refractory Materials: A Series of Monographs”, Academic Press, New York (1971).
2. Storms E.K: “A Critical Review of Refractories”, Los Alamos Scientific Laboratory, New Mexico (1964).
3. Bhuvanewari H.B, Nithiya Priya I, Chandramani R, Rajagopal Reddy V and Mohan Rao G., Studies on zirconium nitride films deposited by reactive magnetron sputtering, *Cryst. Res. Technol.*, 2003, 38, 1047–1051.
4. Fu B and Gao L., Synthesis of nanocrystalline zirconium nitride powders by reduction–nitridation of zirconium oxide, *J. Am. Ceram. Soc.*, 2004, 87, 696–698.
5. Li X.Y, Li G.B, Wang F.J, Ma T.C and Yang D.Z., Investigation on properties of ceramic coatings of ZrN, *Vacuum.*, 1992, 43, 653–656.
6. Schwarz K, Williams A.R, Cuomo J.J, Harper J.H.E and Hentzell H.T.G., Zirconium nitride—a new material for Josephson junctions, *Phys. Rev. B: Condens. Matter.*, 1985, 32, 8312–8316.
7. Sherif El-Eskandaranya M and Ashourb A.H., Mechanically induced gas–solid reaction for the synthesis of nanocrystalline ZrN powders and their subsequent consolidations, *J. Alloys Compd.*, 2000, 313, 224–234.
8. Gu Y, Guo F, Qian Y, Zheng H and Yang Z., A benzene-thermal synthesis of powdered cubic zirconium nitride, *Mater. Lett.*, 2003, 57 (11), 1679–1682.
9. Huang J.H, Ho C.H and Yu G.P., Effect of Nitrogen Flow Rate on the Structure and Mechanical Properties of ZrN Thin Film on Si(100) and Stainless Steel Substrates, *Mater. Chem. Phys.*, 2007, 102, 31–38.

10. Benia H.M, Guemmaz M, Schmerber G, Mosser A and Parlebas J.C., Optical properties of non-stoichiometric sputtered zirconium nitride films, *Appl. Surf. Sci.*, 2003, 211, 146-155.
11. Niu E.W, Li L, Lv G.H, Chen H, Feng W.R, Fan S.H, Yang S.Z and Yang X.Z., Influence of substrate bias on the structure and properties of ZrN films deposited by cathodic vacuum arc, *Mater. Sci. Eng. A.*, 2007, 460–461, 135-139.
12. Sriram S and Chandiramouli R., DFT studies on the stability of linear, ring, and 3D structures in CdTe nanoclusters, *Res Chem Intermed.*, 2013, DOI: 10.1007/s11164-013-1334-6.
13. Valiev M, Bylaska E. J, Govind N, Kowalski K, Straatsma T.P, Van Dam H.J.J, Wang D, Nieplocha J, Apra E, Windus T.L, De Jong W. A NWChem: a comprehensive and scalable open-source solution for large scale molecular simulations. *Comput Phys Commun.*, 2010, 181, 1477–1489.
14. Chandiramouli R., A DFT study on the structural and electronic properties of Barium Sulfide nanoclusters, *Res. J. Chem. Environ.*, 2013, 17, 64-73.
15. Droghetti A, Alfè D, and Sanvito S., Assessment of density functional theory for iron(II) molecules across the spin-crossover transition, *J. Chem. Phys.*, 2012, 137, 124303-124312.
16. Mohammed Bouklah, Houria Harek, Rachid Touzani, Belkheir Hammouti and Yahia Harek., DFT and quantum chemical investigation of molecular properties of substituted pyrrolidinones, *Arabian J. Chem.*, 2012, 5, 163-166.
17. Wei Huang et al., CO chemisorption on the surfaces of the golden cages, *J. Chem. Phys.*, 2009, 131, 234-305.
18. Groenewold Gary S, Gianotto Anita K, McIlwain Michael E, Van Stipdonk Michael J, Kullman Michael, Moore David T, Polfer Nick, Oomens Jos, Infante Ivan, Visscher Lucas, Siboulet Bertrand and de Jong Wibe A., Infrared Spectroscopy of Discrete Uranyl Anion Complexes, *J. Phys. Chem.*, 2008, 112 A, 508-521.
19. Srinivasaraghavan R, Chandiramouli R, Jeyaprakash B.G. and Seshadri S., Quantum chemical studies on CdO nanoclusters stability, *Spectrochim. Acta, Part A.*, 2013, 102, 242-249.
20. John Xavier R and Gobinath E., Experimental and theoretical spectroscopic studies, HOMO–LUMO, NBO and NLMO analysis of 3,5-dibromo-2,6-dimethoxy pyridine, *Spectrochim. Acta, Part A.*, 2012, 97, 215-222.
21. Sriram S, Chandiramouli R, Balamurugan D and A. Thayumanvan., A DFT study on the structural and electronic properties of ZnTe nanoclusters, *Eur. Phys. J. Appl. Phys.*, 2013, 62, 30101.
22. Zhan C.G, Nichols J.A and Dixon D.A., Ionization Potential, Electron Affinity, Electronegativity, Hardness, and Electron Excitation Energy: Molecular Properties from Density Functional Theory Orbital Energies, *J. Phys. Chem.*, 2003, 107 A, 4184-4195.
23. Bandyopadhyay D., Chemisorptions Effect of Oxygen on the Geometries, Electronic and Magnetic properties of small size Nin (n = 1 - 6) Clusters, *J. Mol. Model.*, 2012, 18, 737-749.
24. Sriram S, Chandiramouli R and Jeyaprakash B. G., Influence of fluorine substitution on the properties of CdO nanocluster : a DFT approach, *Struct Chem.*, DOI: 10.1007/s11224-013-0302-5.
25. Dwivedi A and Misra N., Theoretical study of transition metal oxide clusters (TM_nO_m) [(TM- Pd, Rh, Ru) and (n, m =1, 2)], *J. At. Mol. Sci.*, 2012, 3, 297–307.
26. Chandiramouli R, Sriram S and Balamurugan D., *Mol. Phys.*, 2013 , DOI: 10.1080/00268976.2013.805846.
